Cement and Concrete Research 41 (2011) 799–807

Contents lists available at ScienceDirect

Cement and Concrete Research

journal homepage: http://ees.elsevier.com/CEMCON/default.asp

Influence of the cementitious paste composition on the E-modulus and heat of hydration evolutions

Lino Maia [a,*], Miguel Azenha [b], Rui Faria [a], Joaquim Figueiras [a]

[a] LABEST, Laboratory for the Concrete Technology and Structural Behaviour, Faculdade de Engenharia, Universidade do Porto, Rua Dr. Roberto Frias, 4200-465 Porto, Portugal
[b] ISISE, Institute for Sustainability and Innovation in Structural Engineering, Universidade do Minho, Escola de Engenharia, Campus de Azurém, 4800-058 Guimarães, Portugal

ARTICLE INFO

Article history:
Received 22 September 2010
Accepted 21 March 2011

Keywords:
Cement-based pastes (D)
Elastic moduli (C)
Calorimetry (A)

ABSTRACT

E-modulus and heat of hydration are features of cement-based materials that follow a rapid rate of change at early ages. This paper analyses the influence of the composition of cementitious pastes on these features by using two methods: (i) a novel technique for continuously monitoring the E-modulus of cement-based materials, based on evaluating the first resonant frequency of a composite beam containing the material under testing, and (ii) an isothermal calorimeter to determine the released heat of hydration. Seventeen mixes are tested, encompassing pastes with five w/c ratios, as well as different contents of limestone filler, fly ash, silica fume and metakaolin. The results permit the comparison of the E-modulus and heat of hydration sensitivities to mix composition changes, and to check possible relations between these features. This work also helps to establish the technique (i) as a non-destructive method for monitoring the E-modulus evolution in cement-based materials since casting.

© 2011 Elsevier Ltd. All rights reserved.

1. Introduction

Prediction of early-age development of stresses in cement-based materials, as well as evaluation of cracking risks, requires an in-depth knowledge of the mechanical and thermal properties of the materials involved [1–3], including their evolutions right after the setting time. Several test methods can be used for assessing early-age mechanical properties of cement-based materials; however, to undertake continuous monitoring non-destructive techniques are recommended [4,5]. By using acoustic or calorimetry methods, non-destructive tests can be continuously performed, describing the gradual transition from a cementitious paste towards a solid.

Measurements from acoustic methods relate directly to the internal micro-structure of the material, which makes them suitable for monitoring the E-modulus evolution [6].These non-destructive tests have been considerably developed and refined, and nowadays they are based on techniques like ultrasonic pulse velocity, ultrasonic wave reflexion, resonant frequency, impact-echo or acoustic emission [7]. Among these variants, the ultrasonic pulse velocity (compressional waves) and the ultrasonic wave reflexion tests (shear waves) are probably the most commonly used worldwide. However, even though analogies between the ultrasonic wave propagation techniques and the mechanical properties of cement-based materials have been established by several researchers [8–16], most of them faced problems during the early ages [17]. In fact, at the initial stage, when the material is still a suspension of particles in water, the occurrence of air in the test samples influences the compressional wave velocity measurements [18,19]. Furthermore, as shear waves are not transmitted in fluids, their velocities can only be measured upon formation of a percolated-structure in the hardening material [1,16].

Resonant frequency methods are commonly used also to assess the E-modulus of cementitious materials. Usually they are based on the use of longitudinal, transversal and torsional waves [20], but flexural waves may be adopted as well [6]. A variant to these methods was recently proposed by Azenha et al. [21] for continuously monitoring the E-modulus evolution of cement-based materials since casting. In this novel method, termed EMM-ARM (which stands for 'Elasticity Modulus Monitoring through Ambient Response Method'), neither an impact-echo unit nor an electro-mechanical driving unit as described in ASTM C215 [20] are needed, since the use of ambient vibrations (induced by people walking nearby, working machinery, wind, etc.) suffices to excite the specimens under testing. As an outcome of the way it was devised, the EMM-ARM is a fully non-destructive technique, based on the identification of the first resonant flexural frequency of an isostatic composite beam that contains the cement-based material. Then this identified natural frequency is analytically related to the E-modulus of the cementitious material, which allows for a clear identification of the evolution of this elastic property.

The capability of the EMM-ARM to identify different E-modulus kinetics in pastes with accelerating and retarding admixtures was demonstrated in Azenha [22]. But so far its adequacy to capture the influence of the paste composition on the E-modulus evolution has not been tested yet. Accordingly, the present paper will pay particular attention to this issue, and the EMM-ARM will be used to determine

* Corresponding author. Tel.: +351 966096541; fax: +351 225081835.
E-mail addresses: lino.maia@fe.up.pt (L. Maia), miguel.azenha@civil.uminho.pt (M. Azenha), rfaria@fe.up.pt (R. Faria), jafig@fe.up.pt (J. Figueiras).

0008-8846/$ – see front matter © 2011 Elsevier Ltd. All rights reserved.
doi:10.1016/j.cemconres.2011.03.008

the E-modulus evolution in several pastes involving dissimilar additions. These pastes, grouped in 5 sets and in a total of 17 mix compositions, cover the following situations: *(i)* different w/c ratios, *(ii)* adding limestone filler, *(iii)* replacing cement by fly ash, *(iv)* replacing cement by silica fume and *(v)* replacing cement by metakaolin.

For these pastes the released heat of hydration was measured as well with an isothermal calorimeter, towards characterizing the hydration kinetics, which is related to the formation of the solids, and thus to the solid grains assemblage. Thus, it will be possible to compare the evolutions of the E-modulus and of the released heat of hydration, and to identify their sensibilities with respect to composition changes.

2. The used non-destructive measuring methods

2.1. The EMM-ARM

The EMM-ARM has been originally devised for the study of concrete, cast inside an acrylic cylindrical beam with a 92 mm internal diameter and a 1.8 m span. This beam was thereafter placed in simply supported conditions, and continuously subject to modal identification by the use of an accelerometer installed at mid-span [21]. Based on the positive outcomes of this initial implementation, a smaller test set-up aimed attesting mortars and pastes was devised [22]. In this latter variant the acrylic tube is much smaller, with outer/inner diameters of 20 mm/16 mm, and the structural system is a cantilever with a 450 mm span, with an accelerometer placed at the free end.

In the applications of this paper, the lighter version of the EMM-ARM has been used. For clarification, a brief outline of the overall test principle is presented herein. The first step consists in casting the paste to be studied inside the acrylic tube—with one of the extremities closed with a lid–, used as a mould. Then, after properly closing the other extremity of the filled mould, a connection fastening device is attached to the tube and the entire system is fixed and clamped through it, enduring the structural behaviour of a horizontal composite cantilever. An accelerometer is placed at the cantilever's free extremity, to monitor accelerations in the vertical direction induced just by ambient excitation. Fig. 1a depicts a sample during a test run, whilst Fig. 2a schematizes the overall set-up of the EMM-ARM. The specimen size and experimental set-up adopted in this research are almost the same as that of the original implementation [22], except for four details: *(i)* the outer/inner diameters of the acrylic tube are 19.8 mm/15.6 mm (owing to acrylic tube availability), *(ii)* a copper tube is fitted externally to the mould in the neighbourhood of the fastening device, to prevent the acrylic tube from being smashed (in the original version a steel tube was fitted internally), *(iii)* fixation of the accelerometer at the free end of the cantilever is accomplished via an extremity lid made-up of a ring and a nut, to which another nut is glued perpendicularly (see details in Figs. 1b and 2b), shifting the accelerometer's centre 6 mm along the longitudinal axis of the tube, and *(iv)* the other extremity of the acrylic tube is closed with hot glue (which cools down and hardens within seconds), to simplify the handling procedure (see left extremity of Fig. 1a and detail in Fig. 2a).

Fig. 1. a) Experimental set-up in the measuring position for the EMM-ARM; b) accelerometer detail.

The experiment should start as soon as all the components are correctly placed, which usually occurs within ~20 min after mixing the cementitious material. Acceleration measurements are made with a lightweight accelerometer (0.7 g) having a sensitivity of 10 mV/*g* (with 'g' representing acceleration due to gravity), connected to a signal amplifier and a 24-bit data logger, the latter programmed to collect data in packets each of 15-min duration, at a sampling rate of 200 Hz.

No human intervention is necessary throughout the whole experiment, as ambient vibrations that occur in the neighbourhood are intense enough to produce measurable accelerations in the free extremity of the cantilever. The modal identification is performed on the assumption that the ambient vibration can be considered as a white noise (i.e., with equal intensity within the frequency range of interest), and that the resonant frequencies identified with the measured accelerations can be fully related to the response of the analysed structure. An easy way to improve the white noise hypothesis is by using forced ventilation via a domestic fan pointing at the sample. In order to obtain the frequency spectra of the monitored accelerations, and bearing in mind that this is an 'output-only' identification technique, the Welch procedure [23] is adopted to each of the packets of the 15-min acceleration time series. Each of these time series is separated into several sub-sets comprising 4096 data points (with 50% overlapping), and Hanning windows are applied to each sub-set (to reduce leakage effects) [21]. Then a Discrete Fourier Transform is applied to each of these sub-sets, resulting in a group of auto-spectra, which in turn are averaged and normalized according to the procedure described in Ref. [22]. This results in a normalized auto-spectrum that represents the frequency response of the cantilever during the 15-min periods of analysis. An example of such normalized auto-spectrum is shown in Fig. 3, where it is noticeable that the first resonant frequency of the cantilever is around 23.5 Hz.

As the E-modulus of the tested material evolves throughout the experiment, so does the first resonant frequency of the cantilever, and it is illustrative to represent in one graph the power spectra concerning the entire period of testing. This is achieved by plotting all power spectra side-by-side as to create a surface, with the intensity of the spectra being expressed by a colour map as shown in Fig. 4, which allows for a clear identification of the growth of the first resonant frequency along time.

The first resonant frequency *f* of the composite beam can be related to the E-modulus of the cementitious material inside the mould, based on the equation of free vibration of a cantilever. The necessary expressions to finally obtain the E-modulus evolution for the cementitious material are thoroughly explained in Ref. [22], with the final solution of the differential equation of vibration of the composite cantilever shown below:

$$a^3[\cosh(aL)\cos(aL)-1] + \frac{\omega^2 m_1}{EI}[\cos(aL)\sinh(aL)-\cosh(aL)\sin(aL)] = 0 \quad (1)$$

with

$$a = \sqrt[4]{\frac{\omega^2 m}{EI}} \quad \omega = 2\pi f \quad (2)$$

In these equations L is the free span of the cantilever, m is the uniformly distributed mass along the span (due to the acrylic tube and the mix filling it), m_1 is the concentrated mass at the free end (due to the accelerometer and the lid), E is the E-modulus and I is the second moment of area of the composite beam. In Eq. (1) each entry of an identified frequency f of the composite beam corresponds to a unique EI value, since all other variables in the equation are known for a given

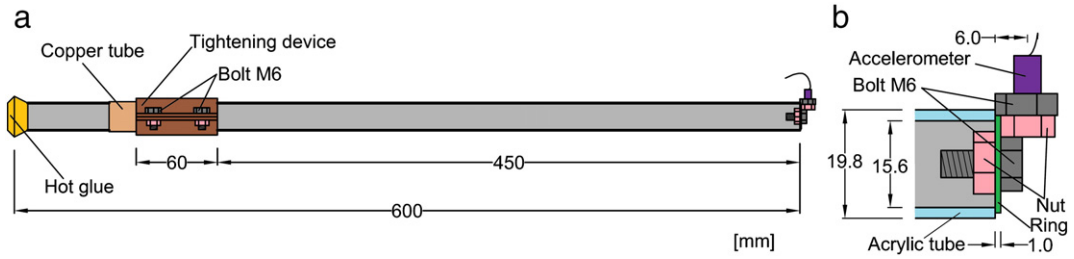

Fig. 2. a) Scheme of the experimental set-up for the EMM-ARM; b) fixation of the accelerometer (vertical cross-section).

experiment. As *EI* can be expressed as the sum of the contributions from the outer acrylic tube and the filling paste under testing, and bearing in mind the internal and external diameters of the acrylic tube, $Ø_i$ and $Ø_e$, as well as the E-modulus of the acrylic, E_a, it is possible to state the E-modulus of the tested paste, E_p, as being [22]:

$$Ep = EI\frac{64}{\pi \varnothing_i^4} - E_a\frac{\varnothing_e^4 - \varnothing_i^4}{\varnothing_i^4} \tag{3}$$

So, by handling Eqs. (1) and (3) it is finally possible to relate the first resonant frequency evolution, identified in Fig. 4, with the E-modulus evolution of the tested cementitious material, as will be done in the experimental program to be presented in Section 3.

2.1.1. Important remarks

Applicability of the formulation to evaluate the E-modulus of the material under testing relies on the assumption that their mass and stiffness are uniformly distributed along the acrylic tube. Therefore, any occurrence of bleeding, segregation, air bubbles or acrylic/paste debonding may negatively affect the measurements and the applicability of the mentioned formulation.

To check fulfilment of the uniform mass distribution along the tube, at the end of each test the composite cantilever should be sawn into at least three parts, and the maximum longitudinal density gradient was assessed by weighing each segment. Measured density gradients higher than 0.5% along the tube, if any, should lead to the rejection of the corresponding test results. In the tests to be presented in Section 3 the density gradient never reached 0.3%, and consequently no test was invalidated.

The issues concerning the possible existence of bleeding and segregation of the cement—although rather unlikely due to the very small height (16 mm) of the cross-section of the material under testing–, as well as to the formation of air bubbles and occurrence of debonding between the acrylic tube and the tested material, should deserve attention as well. The sawn parts of the specimen are to be carefully inspected at the end of each experiment, and in case any of these disturbances is visually detected the corresponding results should be rejected. None of these situations has occurred in the tests to be presented in Section 3.

2.2. The calorimetry

Calorimetry is a well-known method that characterizes the heat release during cement hydration. It is mainly used to quantify the heat of hydration [24–27], to assess the degree of hydration [10,28], to predict maturity [9], and sometimes to estimate physical setting times [29]. Among the many available calorimetric techniques, nowadays results are often obtained with isothermal conduction calorimeters (where the heat flow from a small paste sample is measured under a constant temperature), or with semi-adiabatic calorimeters (where the temperature evolution on the paste sample is monitored, and the energy loss is known). In this investigation a JAF60 isothermal conduction calorimeter was used; further details about this kind of equipment and its measuring principles can be found in Ref. [30].

2.3. Differences between the two methods

Despite both the EMM-ARM and the calorimetry methods providing information related to cement-based material hardening, they are actually measuring different properties. Regarding the EMM-ARM, the results obtained relate directly to the elastic properties of the material, since the growth of the natural frequencies of the composite beam is strictly due to the increase of stiffness of the cementitious material during hardening. Therefore, the EMM-ARM can be very useful to support early-age cracking investigations, especially due to autogenous shrinkage, because this method can identify when the material becomes 'a structure' and how stiff it is along early ages after casting [1].

By measuring the released heat of hydration, calorimetry provides essential information to determine the temperature development at the material level, from which the inherent thermally-induced strains can be assessed. Moreover, measuring the released heat from exothermal chemical reactions is a technique to estimate how much

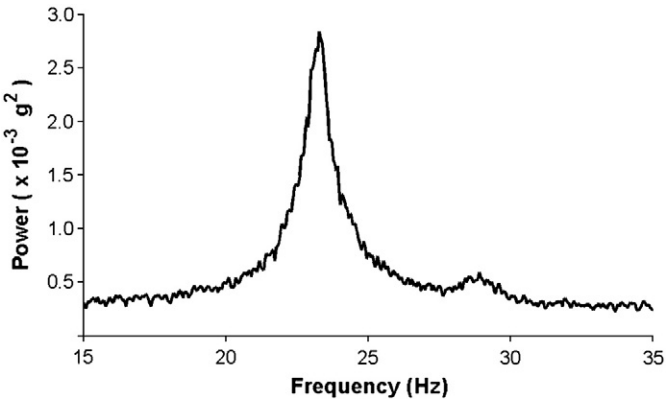

Fig. 3. Example of a normalized auto-spectrum.

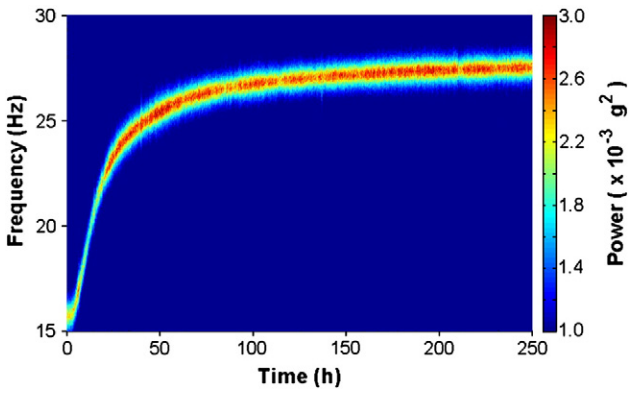

Fig. 4. Example of the colour map of frequency spectra.

reactant has been transformed into reaction products [19].Although most of the chemical reactions involved in the hydration of cementitious pastes produce heat and increase E_p, before structural setting (whilst the paste cannot yet be considered a solid) there are chemical reactions releasing heat but without any E_p increase. Furthermore, neither the released heat of hydration is a direct measure of the solid skeleton formation, nor does the time of solidification correspond to a specific point of the released heat curve [18].

In summary, one can say that the E-modulus evolution is directly related to the development of a percolated solid network (therefore it is concurrent with the volume of assembled solids) [17], whilst the released heat of hydration is far more concerned with the advancement of the chemical reactions (therefore, it can be used to estimate the solid formation) [18,19].

3. Experimental program

3.1. Materials and paste compositions

All the materials used for the paste mixes considered in the experimental program that follows were obtained on the Portuguese market, namely the cement (c) CEM I 42.5R according to EN 197-1 [31], the limestone filler (f), the fly ash (fa), the silica fume (sf), the metakaolin (mtk) and the distilled water (w). All the mixes were made with 320 g of binder (b), the other mix contents being defined in weights according to the ratios specified in Table 1. In this work limestone filler was considered solely as powder (p), whereas fly ash, silica fume and metakaolin were considered as binders. Mix 1 is to be considered the 'reference' one.

Influence of the water-to-cement ratio (w/c) is to be investigated with mixes 1–5, where w/c ranges between 0.30 and 0.50. Keeping w/c constant at 0.45, the influence of the filler-to-cement (f/c) ratio is to be checked with mixes 6–8, with f/c equal to 0.15, 0.30 and 0.45, respectively. Fixing the water-to-binder (w/b) ratio constant at 0.45, influence of the ratio fa/b between the contents of fly ash and total binder (the latter expressed by the sum of the cement and fly ash contents) is to be analysed with mixes 9–11, with fa/b equal to 0.20, 0.40 and 0.60. Regarding the silica fume, three substitution ratios are considered in mixes 12–14, with sf/b equal to 0.05, 0.10 and 0.15. Finally, the effect of partial cement substitution by metakaolin is investigated, with mtk/b ratios of 0.05, 0.10 and 0.15 in mixes 15–17, respectively. It is to be noted that all mixes 6–17 have a constant w/b = 0.45.

Mixes were prepared in plastic containers using a mixer with a vertical paddle, according to the following sequence of procedures: *(i)* water is added to the powders (such instant is named as '$t = 0$'), *(ii)* mixing starts at 500 rpm and extends for 3 min, *(iii)* mixing stops for 2 min, and *(iv)* mixing resumes at 2000 rpm for 2 min. All paste mixes were made twice: one for the EMM-ARM test, and the other for the isothermal calorimeter. In order to evaluate the compressive strengths of the reference mix at different ages, 51 prismatic paste samples ($40 \times 40 \times 160$ mm^3) were prepared and tested following rather closely the norm EN 196-1 [32], but with the ensuing minor changes:

- Batches were prepared using 2140 g of cement;
- Mixing started and extended for 3 min at 'low speed' (paddle rotation: 140 rpm; planetary movement: 62 rpm);
- The mixing then stopped during 2 min;
- Mixing resumed for 2 min at 'high speed' (paddle rotation: 285 rpm; planetary movement: 125 rpm);
- Samples were kept moulded inside a climatic chamber at 20 °C up to the onset of testing.

Table 1
Mix compositions of the pastes used.

Mix	Name	c (g)	f (g)	fa (g)	sf (g)	mtk (g)	w (g)	w/b
1	w/c = 0.45	320					144	0.45
2	w/c = 0.40	320					128	0.40
3	w/c = 0.35	320					112	0.35
4	w/c = 0.30	320					96	0.30
5	w/c = 0.50	320					160	0.50
6	f/c = 0.15	320	48				144	0.45
7	f/c = 0.30	320	96				144	0.45
8	f/c = 0.45	320	144				144	0.45
9	fa/b = 0.20	256		64			144	0.45
10	fa/b = 0.40	192		128			144	0.45
11	fa/b = 0.60	128		192			144	0.45
12	sf/b = 0.05	304			16		144	0.45
13	sf/b = 0.10	288			32		144	0.45
14	sf/b = 0.15	272			48		144	0.45
15	mtk/b = 0.05	304				16	144	0.45
16	mtk/b = 0.10	288				32	144	0.45
17	mtk/b = 0.15	272				48	144	0.45

3.2. Samples to evaluate the E-modulus with the EMM-ARM

In regards to the casting procedure for the composite cantilevers used in the EMM-ARM tests, moulds were initially placed at an inclination of 45° and filled up with paste immediately after the mixing. Upon completion of filling, the acrylic cylinders were carefully vibrated to expel air bubbles, and then the mould tip was closed with hot glue. About 20 min after onset of mixing each cantilever was fixed horizontally at the measuring position, and the accelerometer was screwed to the free end. The first measurements of vertical accelerations started exactly 25 min after '$t = 0$'. Subsequently, measurements were performed continuously for a minimum of 7 days; for some mixes measurements continued even longer, although in discrete form. The experiments were conducted inside a climatic chamber, with controlled temperature and relative humidity at 20.0 ± 0.3 °C and 50 ± 3%, respectively.

Only one sample per mix was tested. However, to check repeatability of the experimental procedure, mixes 1 (w/c = 0.45) and 7 (f/c = 0.30) were performed twice for the EMM-ARM. Rather similar E_p evolutions for each pair of mixes with the same composition were found (in agreement with what was previously noticed in [22]), the maximum differences were found to be 0.35 GPa for mix 1 and 0.30 GPa for mix 7. In addition, for some mixes temperatures inside the acrylic tube were measured to control maturity: the maximum recorded temperature was lower than 21 °C and took place for mix 4 (w/c = 0.30), thus maturity corrections were considered unnecessary.

3.3. Samples to evaluate the heat of hydration with the isothermal calorimeter

For the tests undertaken with the isothermal calorimeter, after mixing pastes were poured inside a plastic bag, which was thereafter carefully sealed by thermoplastic welding. All pastes were studied using samples that contained 30 g of binder. Measurements started 30 min after '$t = 0$', and extended for a minimum of 7 days. Two samples were analysed per mix, and the results presented in this paper correspond to the average of each pair (deviations in the results of each pair were almost negligible, that is, less than 2%). The testing temperature, set at 20 °C, was constant during each experiment.

Heat of hydration results is usually presented in the literature [24–27,33] in terms of the cement weight of the sample (e.g., J/g of cement). This option is pertinent when the research purpose is to specifically analyse the performance of the binder itself (e.g., CEM I 42.5R *versus* CEM I 52.5R). However, in the present paper the purpose is to estimate the hydration progress to assess the performance of dissimilar pastes in terms of solids formation and their assemblage. Thus, in order to compare that to the percolated solid

network and with the E-modulus evolution, it is deemed more adequate to report the released heat of hydration results per m^3 of paste.

4. Results and discussion

4.1. Influence of w/c

Results concerning mixes 1–5, with w/c ranging from 0.30 to 0.50, are shown in Fig. 5 in terms of the E_p evolution evaluated through the EMM-ARM. As expected—having in mind results reported in ultrasonic testing [8,9,13,15,16,34]—it is observed that the w/c ratio has a strong and clear influence on the E-modulus development: E_p starts increasing sooner and reaches higher values for lower w/c ratios. When the E_p at selected ages is related to the mix w/c, this tendency becomes well-defined through the parabolic fittings shown in Fig. 6. Valic [15], who used ultrasonic shear waves reflection, and other authors [12,16,34] that adopted ultrasonic pulse velocity tests, reported similar correlations between the evolution of the paste E-modulus and the w/c ratio.

If attention is now drawn to the influence of w/c on the released heat of hydration per m^3 of paste (see Fig. 7), the latter evaluated in the isothermal calorimeter, one may observe that the evolution curves of the released heat of hydration are much more similar than those in Fig. 5 for the evolution of E_p. In Fig. 7 it is also observed that the released heat of hydration increases as the w/c ratio decreases, as the volumetric cement content is rising concomitantly. However, after ~60 h this trend is not so clear, probably because there is less free water to feed hydration, and the mixing efficiency is smaller for lower w/c ratios (according to Sant et al. [19] isothermal calorimetry is extremely sensitive to mixing).

The test results here presented confirm that the E-modulus evolution has a much more remarkable dependency on the w/c ratio than the heat of hydration. In fact, the E-modulus more than doubles when w/c changes from 0.5 to 0.3, whereas the heat of hydration does not increase more than 30%. A possible explanation for this relies on the fact that for the same amount of hydrated products formed per unit volume (or equivalently, for the same released heat of hydration per m^3), the assemblage of solids is much higher for low w/c ratios.

The joint evolution of the compressive strength and the E-modulus for mix 1 is reproduced in Fig. 8. Standard compressive strength tests (according to Ref. [32]) were performed with the prismatic paste samples mentioned in Section 2.1, at the ages of 12, 16, 20, 24, 30, 36, 42, 48, 60, 72, 96, 132 and 168 h, and at 10, 14, 22 and 42 days. The literature suggests exponential correlations between the compressive strength and the E-modulus [16], or between the compressive strength and ultrasonic measurements [11,13]. Adopting an exponential fitting in Fig. 8 a coefficient of correlation $R^2 = 0.982$ was found, which supports its appropriateness to express the dependency between E_p and the compressive strength.

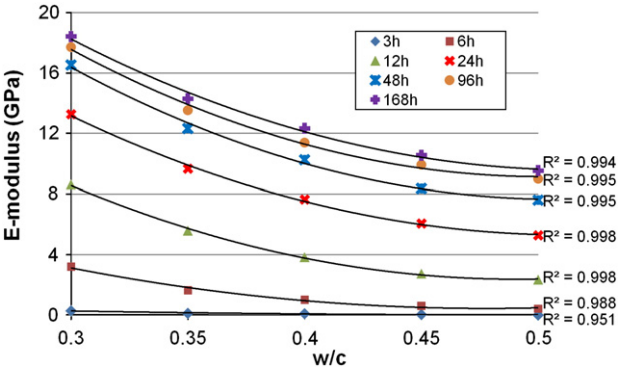

Fig. 6. E_p *vs.* w/c ratio at different ages (parabolic fitting).

4.2. Influence of limestone filler content

Influence of limestone filler content on the E-modulus and heat of hydration evolutions of mixes 1 and 6–8, with f/c ratios ranging from 0 to 0.45 (all mixes with w/c = 0.45), can be analysed in Figs. 9 and 10, respectively. In Fig. 9 it can be noticed that even a small addition of limestone filler (f/c = 0.15) causes the E-modulus to reach higher values and increase faster at early ages than with f/c = 0 (reference mix). Moreover, it is observed that larger additions of limestone filler (f/c = 0.30 and f/c = 0.45) produce even higher E-moduli and growth rates. Probably such a tendency is due to the fact that decreasing the water-to-powder ratio leads to pastes with higher compactness and enhanced assemblage [35]. Nonetheless, and bearing in mind the evolution of E_p with f/c, the increasing effect in the attained E_p is more visible between f/c = 0 and f/c = 0.15 than what occurs for larger f/c ratios.

In Fig. 10 it is observed that the released heat of hydration increases with the limestone filler content up to the age of 12 h, and that the dormant period shortens [25,35]. Conversely, at later ages the limestone filler seems to have an attenuating influence on the released heat of hydration, pointing to some increase of the dilution effect of clinker. However, small additions of limestone filler (e.g., f/c = 0.15) seem to have a negligible influence on the released heat of hydration. This is in agreement with findings of Lothenbach et al. [35], who reported that limestone filler has some pozzolanic activity, which partially cancels the dilution effect of clinker.

Finally, comparing Fig. 9 with Fig. 10 it can be said that the E-modulus is very sensitive to limestone filler additions for similar values of released heat of hydration. For instance, at the age of 15 h

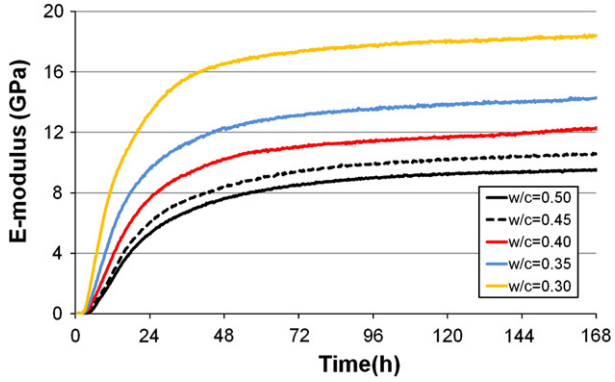

Fig. 5. Influence of w/c ratio on the E_p evolution.

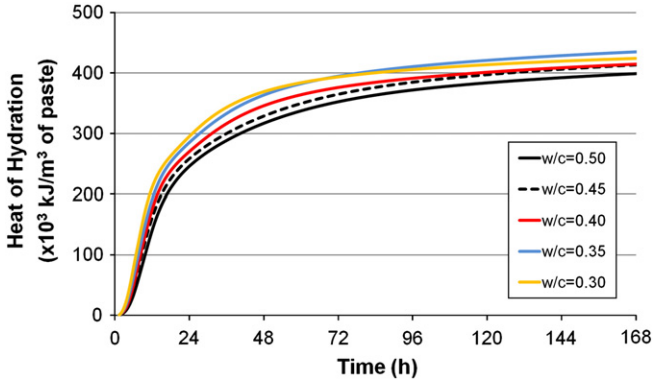

Fig. 7. Influence of w/c ratio on the released heat of hydration.

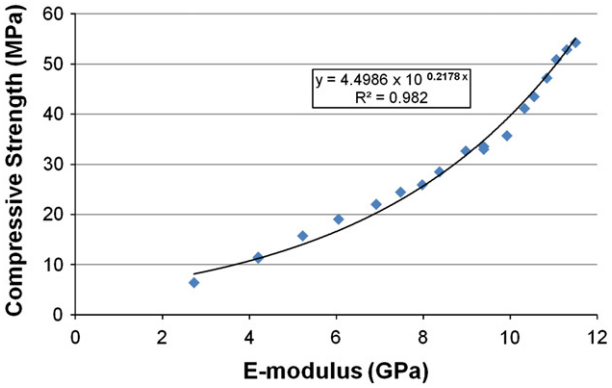

Fig. 8. Fitting the compressive strength as a function of E_p for mix 1.

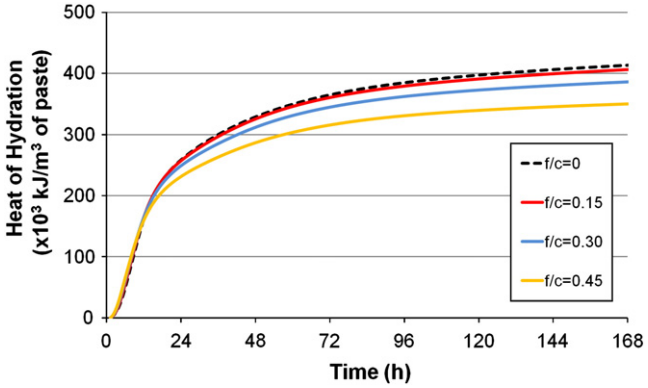

Fig. 10. Influence of limestone filler content on the released heat of hydration (w/c = 0.45).

the released heat of hydration is similar for all mixes—indicating identical amounts of hydrated products, but the volume of assembled solid is obviously greater for pastes with higher f/c, as evidenced by the increased E-moduli that were obtained.

4.3. Influence of fly ash content

Relevance of cement substitution by fly ash on the evolution of E_p during the first 7 days after casting is illustrated in Fig. 11, involving mixes 1 and 9–11. This figure shows that, in comparison to the reference mix, the paste with fa/b = 0.20 causes almost negligible effects on the E-modulus evolution during the first 7 days (168 h). A slight delay on the E-modulus evolution is observable up to the age of 24 h, but a small increase in the evolution rate is observed after 80 h. For higher values of fa/bit is clear that a remarkable delay on the E_p evolution takes place at early ages. At later ages a strong decrease of the E-modulus is detected for higher substitutions, especially for fa/b = 0.60. However, slightly higher increasing rates are observed at these later ages, which is probably due to the pozzolanic activity, as reported in Frías et al. [26]. Looking at Fig. 12, where the E-modulus evolution is presented as a function of fa/b up to the age of 60 days, one observes that after 96 h the E-modulus increases more for higher fly ash contents. In addition, the parabolic fitting in Fig. 12, showing R^2values very close to 1.0, indicates also another interesting feature: by increasing the age the maximum of each parabolic curve is reached at higher fa/b ratios (e.g., for the age of 96 h E_p is maximized at fa/b ~ 0.10, whereas for the age of 60 days E_p is maximized at fa/b ~ 0.20). These results are in agreement with tendencies reported in Ref. [36] (for concretes) and in Ref. [28] (for mortars).

Regarding the total released heat of hydration, plotted along time in Fig. 13, one observes that it strongly decreases when the cement replacement by fly ash increases, as also reported in the literature [24,26–28]. Different from the E_p evolution with fa/b, the decrease of the released heat of hydration per unit volume is roughly equivalent to the amount of cement substituted, so increasing the fly ash content enforces mainly the dilution effect.

4.4. Influence of silica fume content

The importance of silica fume as a partial substitution for cement on the E-modulus evolution may be analysed in Fig. 14, where mixes 1 and 12–14 are involved. It is possible to confirm that all mixes with silica fume exhibit E-modulus evolutions that surpass the one of the reference mix. However, with sf/b = 0.10 the E-modulus increase in comparison to the reference mix is less than that for sf/b = 0.05, and with sf/b = 0.15 a further drop of E_p is observed in comparison to the E-modulus concerning sf/b = 0.10. This points to the evidence that some 'saturation' in the benefits of using silica fume is obtained for sf/b ~ 0.05, as far as the improvement of E_p is concerned.

A better defined and simpler tendency is found in Fig. 15, where a progressive reduction of the released heat of hydration with the increase of cement replacement by silica fume is observable. This suggests that the chemical reactions in which silica fume is involved give a low contribution to the heat of hydration, as also reported in Ref. [33] for a mix with 10% of cement replacement by silica fume at the age of 72 h. However, different results were found by other authors [26,37], who reported that the released heat of hydration was higher for sf/b = 0.10 and lower for sf/b = 0.30, compared to a reference mix with only cement as binder. This points to some peculiarities of the silica fume used in this research, which could only be clarified exactly upon physical and chemical characterizations;

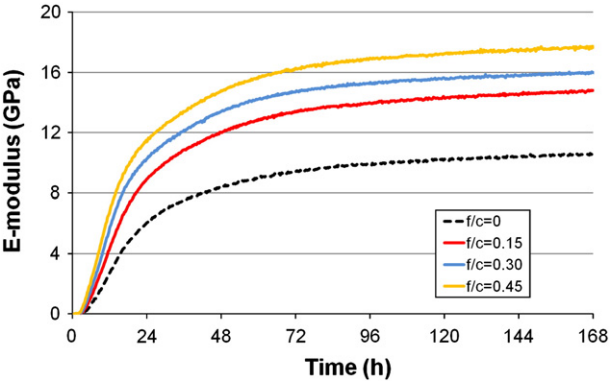

Fig. 9. Influence of limestone filler content on the E_p evolution (w/c = 0.45).

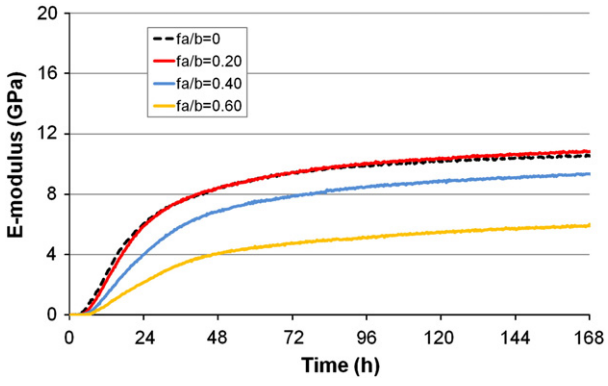

Fig. 11. Influence of fly ash content on the E_p evolution (w/b = 0.45).

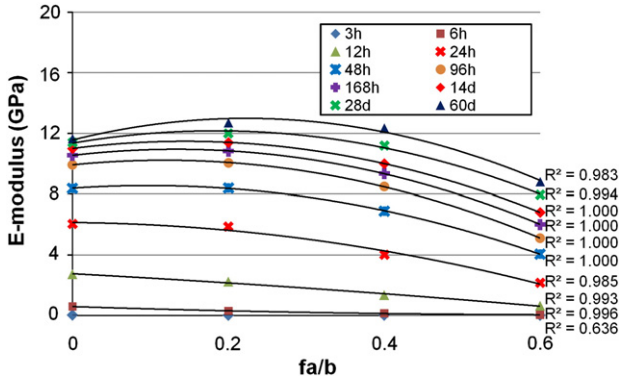

Fig. 12. E_p *vs.* fa/b at different ages (parabolic fitting, w/b = 0.45).

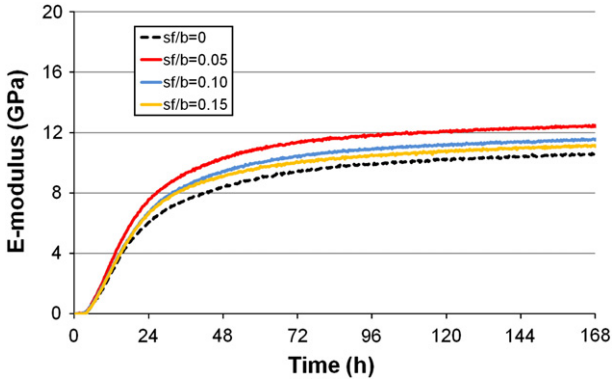

Fig. 14. Influence of silica fume content on the E_p evolution (w/b = 0.45).

unfortunately, within the scope of this research it was not possible to undertake such characterizations.

4.5. Influence of metakaolin content

Fig. 16 allows for checking the influence of metakaolin content on the evolution of E_p, by considering mixes 1 and 15–17. In comparison to what is observed for the reference mix (mtk/b = 0), the E-moduli are superior at all ages when some cement replacement by metakaolin is present. Comparing this observation with the literature, ultrasonic pulse velocities in concretes with mtk/b ratios equal to 0.05, 0.10 and 0.15 were almost always found to be greater than the ones for a mix with mtk/b = 0 [36,38]. In Fig. 16 it is also observed that up to the age of 12 h the greater the mtk/b ratio the higher becomes the E-modulus; however, for later ages (particularly between 12 and 96 h) small mtk/b ratios—between 0.05 and 0.10—induce the highest E-moduli.

In Fig. 17 it is observed that the evolutions of the released heat of hydration for mixes with mtk/b = 0.05 and mtk/b = 0.10 are almost indistinguishable. The mix with mtk/b = 0.15, although exhibiting the highest released heat of hydration at the age of 7 days, it is associated to the lowest values within the interval 20–80 h. In a heat flow differential calorimeter Snelson et al. [27] reported identical observations for the same mtk/b ratios. Moreover, in Fig. 17 it is observed that for mtk/b up to 0.10, and until the age of 96 h, the pozzolanic activity and the dilution effects compensate each other. Although for different ratios, this observation is consistent with findings reported by Frías et al. [26]. Finally, up to the age of 96 h the dilution effect is visible in Fig. 17 for the mix with mtk/b = 0.15; for later ages the pozzolanic activity is visible for all mtk/b ratios.

4.6. Final remarks on the different pastes

Comparing the E-moduli reported in Figs. 5 and 9 at the age of 7 days, and for the paste mixes 1–5 and 6–8, interesting observations can be drawn on the basis of the w/p and f/c ratios (bearing in mind that for mixes 1–5 one has w/p = w/c, and that for mixes 6–8 an increase of f/c leads to a decrease of w/p):

- With an almost constant w/p the growth on the E-modulus was more strongly influenced by raising the limestone filler content than that of the cement. For instance, mix 2 (w/p = 0.40, f/c = 0) led to a paste with E_p = 12.3 GPa, whilst in mix 6 (w/p = 0.39, f/c = 0.15) the E_p reached 14.8 GPa. Likewise, for mix 3 (w/p = 0.35, f/c = 0) an E_p = 14.3 GPa was obtained, whereas for mix 7 (w/p = 0.35, f/c = 0.30) the E-modulus increased to E_p = 16.0 GPa.
- However, for the mixes with the lowest w/p ratios the previous tendency was not observed. In fact, mix 8 (w/p = 0.31, f/c = 0.45) had the largest limestone filler content and led to a paste with E_p = 17.7 GPa, which is inferior to the value of E_p = 18.4 GPa from mix 4, with practically the same w/p (= 0.30) but with f/c = 0.

Therefore, to improve the E-modulus it is more efficient to reduce the w/p ratio by adding limestone filler, than by decreasing w/c (especially for low limestone filler contents). Furthermore, adding limestone filler is more economical and reduces the released heat of hydration, which are further advantages when compared to adding cement.

Analysing the influences of fly ash (mixes 9–11) and silica fume (mixes 12–14), in Figs. 11–15 some similarities are noticeable, despite different contents having been used. With both additions the dilution effect seemed to play the main role, as far as the released heat of hydration is concerned, whereas the pozzolanic activity was rather

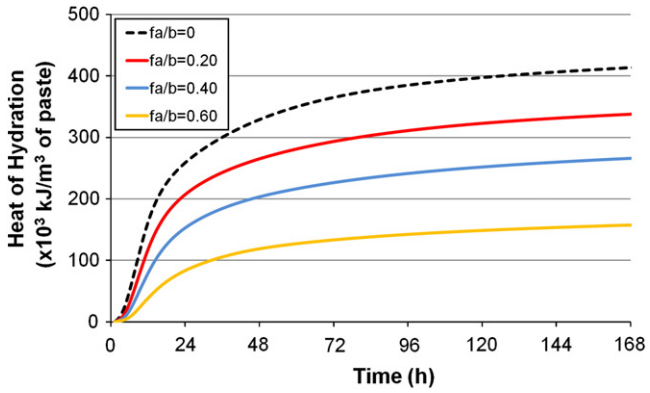

Fig. 13. Influence of fly ash content on the released heat of hydration (w/b = 0.45).

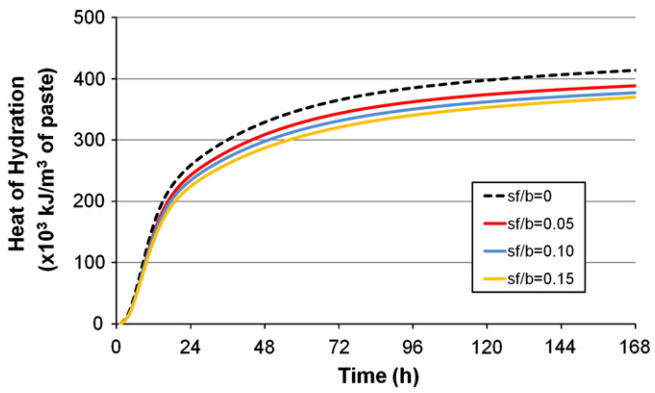

Fig. 15. Influence of silica fume content on the released heat of hydration (w/b = 0.45).

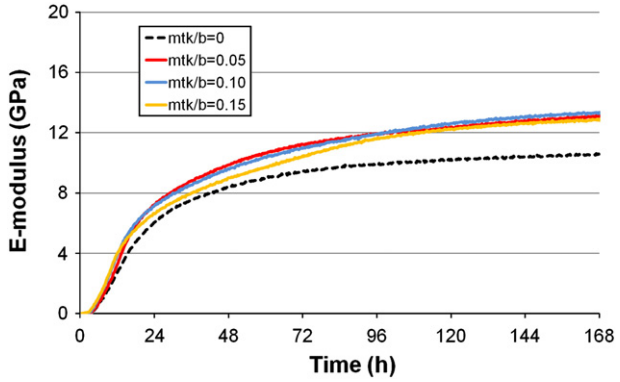

Fig. 16. Influence of metakaolin content on the E_p evolution (w/b = 0.45).

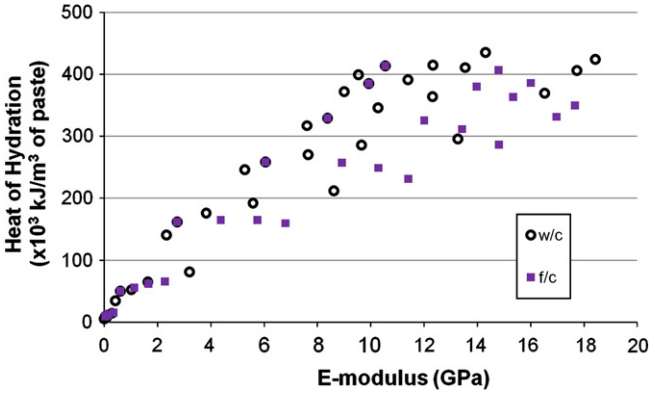

Fig. 18. E-modulus *vs.* released heat of hydration during the first 7 days (mixes 1–8).

more important for the E-modulus development. Influence of the pozzolanic activity on the E_p evolution was more important during the first 7 days with silica fume, whilst with fly ash it was dominant at later ages, in accordance with what is reported in Ref. [26]. Comparing the influences of silica fume (mixes 12–14) and metakaolin (mixes 15–17), it was observed that metakaolin engenders higher pozzolanic activity, especially for later ages.

As referred in Section 2.3, the EMM-ARM and the calorimetry methods provide information related to different material features. The EMM-ARM evaluates the E-modulus, an elastic property closely linked to the material micro-structure, whilst calorimetry characterises the released heat of hydration, which is strictly concerned with the chemical reactions involved. Nevertheless, as the evolution of E_p is a consequence of the hydration chemical reactions, in Fig. 18 it is interesting to follow the joint progression of E_p with the released heat of hydration, obtained at the ages of 3, 6, 12, 24, 48, 96 and 168 h, and for mixes 1–8 (with different w/p involved).In Fig. 19 a similar representation is made, but now for mixes 1 and 9–17 (all with w/p = 0.45).

Generally speaking, in Fig. 18 one observes that the results fall within a limited band, indicating that the evolution of one property induces the increase of the other. However, no general and single correlation can be established for mixes with different w/p ratios. In fact a large scatter is visible, expressed by the fact that for a given value of the heat of hydration the corresponding E-modulus may vary more than 100%.

Conversely, in Fig. 19 a linear fitting correlates rather well with the results concerning mix 1 (where cement was the unique binder) and mixes 9–17 (where cement was partially replaced by fly ash, silica fume or metakaolin). For all these mixes, and up to the age of 7 days, an increase of $E_p = 1$ GPa occurs for an increase in the released heat of hydration of circa 30×10^3 kJ/m^3. Furthermore, the linear fitting indicates that the E-modulus ceases to be null only after some heat of hydration has been released (about$15–20 \times 10^3$ kJ/m^3), which is consistent to what is to be expected. Therefore, one can conclude that for mixes with a similar solid content (expressed by the same w/p), the released heat of hydration can be used to estimate the micro-structure (or solid) formation, and that the E-modulus increases linearly with the solid formation and its assemblage.

5. Conclusions

From the results presented in this paper the following conclusions can be drawn:

- The EMM-ARM proved to be a feasible method for tracing the continuous E-modulus evolution, having enough sensibility to detect changes due to different cementitious paste compositions.
- An exponential correlation between the E-modulus and the compressive strength was found for the cement paste with w/c = 0.45.
- The clinker content played the main role in the released heat of hydration, when cement was partially replaced by fly ash or silica fume. However, influences of fly ash and silica fume on the E-modulus were dissimilar: whilst silica fume induced a higher E-modulus at all ages, the use of fly ash delayed and reduced the evolution of E-modulus at early ages, and lead to higher values at later ages. The pozzolanic activity of the metakaolin cancelled the dilution effect of clinker, regarding the released heat of hydration at early ages. However, the E-modulus was enhanced by using metakaolin as a substitute for cement.
- The water-to-powder ratio (w/p) had a strong influence on the E-modulus evolution. For a lower w/p ratio, the volume of assembled

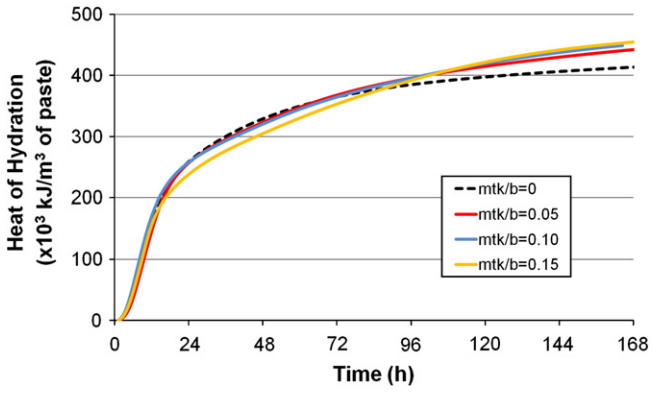

Fig. 17. Influence of metakaolin content on the released heat of hydration (w/b = 0.45).

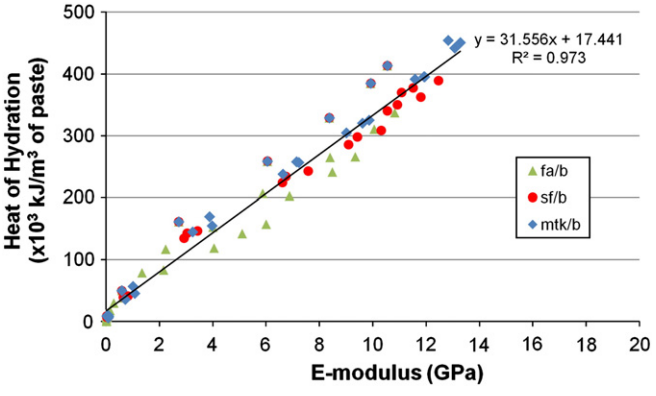

Fig. 19. E-modulus *vs.* released heat of hydration during the first 7 days (mixes 1 and 9–17).

solid grains is higher for the same released heat of hydration (i.e., for the same amount of products formed). Furthermore, decreasing w/p by adding limestone filler was more efficient to increase the E-modulus evolution than by adding cement, particularly for low contents. In addition, adding limestone filler reduces heat of hydration production, which constitutes a further advantage compared to adding cement.

– Up to the age of 7 days, and for mixes with just cement or cement partially replaced by fly ash, silica fume or metakaolin (all the mixes with w/p = 0.45), an almost linear correlation was found between the E-modulus and the released heat of hydration. Therefore, for mixes with the same w/p ratio the volume of connected solid grains controls the E-modulus evolution.

Acknowledgments

Funding provided by the Portuguese Foundation for Science and Technology (FCT) and the European Social Fund (ESF), namely for the Research Projects PTDC/ECM/70693/2006 and PTDC/ECM/099250/2008, and to the first author through the PhD grant SFRH/BD/24427/2005, is gratefully acknowledged.

References

[1] RILEM TC 181-EAS, Early Age Cracking in Cementitious Systems—Report of RILEM Technical Committee 181-EAS—Early Age Shrinkage Induced Stresses and Cracking in Cementitious Systems, RILEM Publications SARL, 2003.
[2] RILEM TC 119-TCE, Prevention of thermal cracking in concrete at early ages—Recommendations of TC 119-TCE—avoidance of thermal cracking in concrete at early ages E& FN Spon, 1998.
[3] ACI 231R-10, Report on early-age cracking, Causes, Measurement, and Mitigation, Reported by ACI Committee, 231, 2010, ACI.
[4] V.M. Malhotra, N.J. Carino, Handbook on Nondestructive Testing of Concrete, Second ed.CRC Press, Washington, D.C., 2004.
[5] RILEM TC-185-ATC, in: H.W. Reinhardt, C.U. Grosse (Eds.), Advanced Testing of Cement-Based Materials during Setting and Hardening—Final Report of RILEM TC 185-ATC, RILEM Publications SARL, Bagneux, France, 2005.
[6] N. Swamy, G. Rigby, Dynamic properties of hardened paste, mortar and concrete, Materials and Structures 4 (1971) 13–40.
[7] T. Voigt, The application of an ultrasonic shear wave reflection method for nondestructive testing of cement-based materials at early ages: An experimental and numerical analysis, University of Leipzig, Germany, Books on Demand, Norderstedt (PhD Thesis), 2005.
[8] H.W. Reinhardt, C.U. Grosse, Continuous monitoring of setting and hardening of mortar and concrete, Construction and Building Materials 18 (2004) 145–154.
[9] T. Voigt, S.P. Shah, Properties of early-age portland cement mortar monitored with shear wave reflection method, ACI Materials Journal 101 (2004) 473–482.
[10] M. Krauß, K. Hariri, Determination of initial degree of hydration for improvement of early-age properties of concrete using ultrasonic wave propagation, Cement & Concrete Composites 28 (2006) 299–306.
[11] T. Voigt, Z. Sun, S.P. Shah, Comparison of ultrasonic wave reflection method and maturity method in evaluating early-age compressive strength of mortar, Cement & Concrete Composites 28 (2006) 307–316.
[12] H.K. Lee, K.M. Lee, Y.H. Kim, H. Yim, D.B. Bae, Ultrasonic in-situ monitoring of setting process of high-performance concrete, Cement and Concrete Research 34 (2004) 631–640.
[13] Y. Lin, S.-F. Kuo, C. Hsiao, C.-P. Lai, Investigation of pulse velocity-strength relationship of hardened concrete, ACI Materials Journal 104 (2007) 344–350.
[14] K. Subramaniam, J. Lee, Ultrasonic assessment of early-age changes in the material properties of cementitious materials, Materials and Structures 40 (2007) 301–309.
[15] M.I. Valic, Hydration of cementitious materials by pulse echo USWR: method, apparatus and application examples, Cement and Concrete Research 30 (2000) 1633–1640.
[16] A. Boumiz, C. Vernet, F.C. Tenoudji, Mechanical properties of cement pastes and mortars at early ages: evolution with time and degree of hydration, Advanced Cement Based Materials 3 (1996) 94–106.
[17] D.P. Bentz, A review of early-age properties of cement-based materials, Cement and Concrete Research 38 (2008) 196–204.
[18] M. Dehadrai, G. Sant, D. Bentz, J. Weiss, Identifying the fluid-to-solid transition in cementitious materials at early ages using ultrasonic wave velocity and computer simulation, Concrete International 259 (2009) 66–76.
[19] G. Sant, M. Dehadrai, D. Bentz, P. Lura, C.F. Ferraris, J.W. Bullard, J. Weiss, Detecting the fluid-to-solid transition in cement pastes, Concrete International 31 (2009) 53–58.
[20] ASTM C 215, Standard test method for fundamental transverse, longitudinal, and torsional resonant frequencies of concrete specimens, American Society for Testing and Materials, Philadelphia, PA, 2002.
[21] M. Azenha, F. Magalhães, R. Faria, Á. Cunha, Measurement of concrete E-modulus evolution since casting: a novel method based on ambient vibration, Cement and Concrete Research 40 (2010) 1096–1105.
[22] M. Azenha, Numerical simulation of the structural behaviour of concrete since its early ages, PhD Thesis, Faculty of Engineering - University of Porto, Porto, 2009.
[23] P. Welch, The use of fast Fourier transform for the estimation of power spectra: a method based on time averaging over shortmodified periodograms, IEEE Transaction on Audio and Electro-Acoustics 15 (2) (1967).
[24] B.W. Langan, K. Weng, M.A. Ward, Effect of silica fume and fly ash on heat of hydration of Portland cement, Cement and Concrete Research 32 (2002) 1045–1051.
[25] A.-M. Poppe, G. De Schutter, Cement hydration in the presence of high filler contents, Cement and Concrete Research 35 (2005) 2290–2299.
[26] M. Frías, M.I.S. de Rojas, J. Cabrera, The effect that the pozzolanic reaction of metakaolin has on the heat evolution in metakaolin-cement mortars, Cement and Concrete Research 30 (2000) 209–216.
[27] D.G. Snelson, S. Wild, M. O'Farrell, Heat of hydration of Portland cement-metakaolin-fly ash (PC-MK-PFA) blends, Cement and Concrete Research 38 (2008) 832–840.
[28] N. Robeyst, C.U. Grosse, N. De Belie, Measuring the change in ultrasonic p-wave energy transmitted in fresh mortar with additives to monitor the setting, Cement and Concrete Research 39 (2009) 868–875.
[29] K. Wang, Z. Ge, J. Grove, J. Mauricio Ruiz, R. Rasmussen, T. Ferragut, Developing a simple and rapid test for monitoring the heat evolution of concrete mixtures for both laboratory and field applications, Center for Transportation Research and Education, Iowa State University, 2007.
[30] L. Wadsö, An experimental comparison between isothermal calorimetry, semi-adiabatic calorimetry and solution calorimetry for the study of cement hydration, NORDTEST report TR 522, 2003.
[31] EN 197–1:2000, Cement—Part 1: Composition, Specifications and Conformity Criteria for Common Cements, 2000.
[32] EN 196-1, (European Norm)—Methods of Testing Cement, Part 1: Determination of Strength, 2005.
[33] Y. Zhang, W. Sun, S. Liu, Study on the hydration heat of binder paste in high-performance concrete, Cement and Concrete Research 32 (2002) 1483–1488.
[34] G. Trtnik, G. Turk, F. Kavcic, V.B. Bosiljkov, Possibilities of using the ultrasonic wave transmission method to estimate initial setting time of cement paste, Cement and Concrete Research 38 (2008) 1336–1342.
[35] B. Lothenbach, G. Le Saout, E. Gallucci, K. Scrivener, Influence of limestone on the hydration of Portland cements, Cement and Concrete Research 38 (2008) 848–860.
[36] E. Güneyisi, M. Gesoğlu, Properties of self-compacting mortars with binary and ternary cementitious blends of fly ash and metakaolin, Materials and Structures 41 (2008) 1519–1531.
[37] E.-H. Kadri, R. Duval, Hydration heat kinetics of concrete with silica fume, Construction and Building Materials 23 (2009) 3388–3392.
[38] M. Gesoğlu, Influence of steam curing on the properties of concretes incorporating metakaolin and silica fume, Materials and Structures 43 (2010) 1123–1134.